Purinergic Signalling (2023) 19:29–41
https://doi.org/10.1007/s11302-022-09844-8

ORIGINAL ARTICLE

Dorsal root ganglia P2X4 and P2X7 receptors contribute to diabetes-induced hyperalgesia and the downregulation of electroacupuncture on P2X4 and P2X7

Qun-qi Hu[1] · Xiao-fen He[1] · Yi-qi Ma[1] · Li-qian Ma[1] · Si-ying Qu[1] · Han-zhi Wang[1] · Yu-rong Kang[1] · Lu-hang Chen[1] · Xiang Li[1] · Bo-yu Liu[1] · Xiao-mei Shao[1] · Jun-fan Fang[1] · Yi Liang[1] · Jian-qiao Fang[1] · Yong-liang Jiang[1]

Received: 28 August 2021 / Accepted: 11 January 2022 / Published online: 26 February 2022

Abstract

Diabetic neuropathic pain (DNP) is highly common in diabetes patients. P2X receptors play critical roles in pain sensitization. We previously showed that elevated P2X3 expression in dorsal root ganglion (DRG) contributes to DNP. However, the role of other P2X receptors in DNP is unclear. Here, we established the DNP model using a single high-dose streptozotocin (STZ) injection and investigated the expression of P2X genes in the DRG. Our data revealed elevated P2X2, P2X4, and P2X7 mRNA levels in DRG of DNP rats. The protein levels of P2X4 and P2X7 in DNP rats increased, but the P2X2 did not change significantly. To study the role of P2X4 and P2X7 in diabetes-induced hyperalgesia, we treated the DNP rats with TNP-ATP (2',3'-O-(2,4,6-trinitrophenyl)-adenosine 5'-triphosphate), a nonspecific P2X1–7 antagonist, and found that TNP-ATP alleviated thermal hyperalgesia in DNP rats. 2 Hz electroacupuncture is analgesic against DNP and could downregulate P2X4 and P2X7 expression in DRG. Our findings indicate that P2X4 and P2X7 in L4–L6 DRGs contribute to diabetes-induced hyperalgesia, and that EA reduces thermal hyperalgesia and the expression of P2X4 and P2X7.

Keywords Diabetic neuropathic pain · DRG · P2X4 · P2X7 · TNP-ATP · Electroacupuncture

Abbreviations

ATP	Adenosine 5′-triphosphate
AUC	Area under the curve
BW	Body weight
DNP	Diabetic neuropathic pain
DRG	Dorsal root ganglion
EA	Electroacupuncture
FBG	Fasting blood glucose
GAPDH	Glyceraldehyde-3-phosphate dehydrogenase
IF	Immunofluorescence
i.p.	Intraperitoneal
NS	Normal saline
P2X	Purinergic ligand-gated cationic channel
RT-qPCRs	Real-time quantitative polymerase chain reactions
PWL	Paw withdrawal latency
SD	Standard deviation
STZ	Streptozotocin
TNP-ATP	2',3'-O-(2,4,6-trinitrophenyl)-adenosine 5'-triphosphate
WB	Western blotting

Introduction

Diabetes is a leading health burden worldwide [1] and affects about 415 million people, with the number predicted to rise to 700 million by 2045 [2]. In diabetics, hyperglycemia and vascular impairment contribute to the neuronal dysfunction in the peripheral nervous system [3, 4]. In view of the high prevalence of diabetes worldwide, diabetic neuropathic pain (DNP) has become a relatively frequent disease [5, 6] that affects 11–21% of diabetics and is characterized by aberrant pain sensation, including hyperalgesia, spontaneous pain,

Qun-qi Hu, Xiao-fen He and Yi-qi Ma contributed equally.

✉ Jian-qiao Fang
fangjianqiao7532@163.com

✉ Yong-liang Jiang
jyl2182@126.com

[1] Key Laboratory of Acupuncture and Neurology of Zhejiang Province, Department of Neurobiology and Acupuncture Research, The Third Clinical Medical College, Zhejiang Chinese Medical University, Hangzhou, Zhejiang 310053, People's Republic of China

and allodynia [7–9]. Despite being the major symptom of diabetic neuropathy, the pathogenesis of DNP is still not fully understood.

P2X receptors are ligand-gated ion channels assembled into homotrimers or heterotrimers [10]. There are 7 known P2X receptors with 35–48% homology. P2X receptors are generally activated by adenosine 5′-triphosphate (ATP) and are involved in various physiologic and pathophysiologic processes, including inflammation and pain [11]. Since the identification of the link between injection of adenosine compounds into human skin blisters and pain initiation in 1977 [12], numerous studies have found that the activation of P2X receptors causes pain-related reactions in animals [13–16]. We previously reported the relationship between pain sensitization and P2X3 in dorsal root ganglia (DRG) of DNP rats [17, 18]. However, systematic studies of the involvement of other P2X receptors in DNP are lacking.

DNP is usually managed by using analgesics, like duloxetine, pregabalin, and opioids [19, 20], but these are not always effective and have significant side effects. Clinically, electroacupuncture (EA) is employed to treat various chronic pain disorders [21–24] and has potential use in DNP treatment [25]. However, the mechanisms underlying the effect of EA against DNP are not clear. Here, we used a rat model of streptozocin (STZ)-triggered DNP, and examined mRNA expression of P2X1–2 and P2X4–7 receptors in DRG at diverse times after STZ administration. Western blot (WB) and immunofluorescence (IF) were then used to investigate the protein expression of receptors with elevated mRNA content. The influences of EA on DNP rats and the expression of P2X4 and P2X7 in DRG after EA treatment were evaluated.

Materials and methods

Animals

Male Sprague–Dawley rats (200 ± 20 g) were bought from Shanghai Slac Laboratory Animal Co., Ltd (SCXK (hu) 2017–0005) and housed at Animal Laboratory Center of Zhejiang Chinese Medical University (SYXK (zhe) 2018–0012). Five rats per cage were housed under controlled conditions (20–24 °C, 40–60% relative humidity, and 12 h light/dark cycles) and free access to food and water. The rats were adapted to the new environment for 1 week before. Animal experiment protocols were approved by the animal welfare committee of Zhejiang Chinese Medical University (IACUC-20190805–04).

Generation of the DNP rat model

Rats were fasted for 16 h before intraperitoneal (i.p.) injection with 65 mg/kg of STZ (S0130, Sigma) in citrate buffer (0.1 mol/L, pH 4.5) [26, 27]. Rats in DNP group, DNP + normal saline group (DNP + NS group), DNP + TNP-ATP 50 nmol group, and DNP + TNP-ATP 100 nmol group were intraperitoneally inoculated with STZ, while control group (Ctrl group) and control + normal saline group (Ctrl + NS group) rats received an equal volume of vehicle. Fasting blood glucose (FBG) was measured 7 days after STZ inoculation. Rats with FBG content > 13.9 mmol/L [28] and thermal hyperalgesia considered to be successful DNP models.

Experimental groups

There were 3 experiment types. In experiment type 1, rats were assigned at random into a Ctrl group ($n = 16$), with tissues being collected 21 days after STZ injection, and a DNP group ($n = 56$). Of those in the DNP group, 16 rats were sacrificed for tissues 7 days after STZ administration, 16 were sacrificed 14 days after administration, 16 were sacrificed at 21 days after administration and tissues collected, four rats died, and four were modeled unsuccessfully. Body weight (BW), FBG, and paw withdrawal latency (PWL) were examined as per the schedule on Fig. 1a. Changes in mRNA and protein levels of P2X1–2 and P2X4–7 receptors in DRG were assessed at various DNP stages.

In experiment type 2, the involvement of P2X4 and P2X7 in DNP was assessed by treating the rats with TNP-ATP (2',3'-O-(2,4,6-trinitrophenyl)-adenosine 5'-triphosphate), a nonspecific antagonist of P2X receptors. Twenty-four rats were randomly divided into a Ctrl + NS, a DNP + NS, a DNP + TNP-ATP 50 nmol, and a DNP + TNP-ATP 100 nmol group, 6 rats per group. One rat died and two were modeled unsuccessfully. Rats in DNP + TNP-ATP 50 nmol and DNP + TNP-ATP 100 nmol group were treated with reduplicative administrations from 15 to 21 days after STZ injection, while other groups received an equal volume of normal saline (NS). The BW, FBG, and PWL of all rats were recorded as outline in Fig. 5a.

Experiment type 3 assessed the influences of EA on DNP and P2X4, P2X7 in DRG. Rats were randomly divided into a Ctrl, a DNP, and a DNP + EA group (16 rats for each group). Four rats were modeled unsuccessfully. Rats in DNP + EA group received EA treatment from 15 to 21 days after STZ injection, once a day. BW, FBG, and PWL tests were done as outline in Fig. 6a and tissues from all group rats were collected 21 days post administration of STZ.

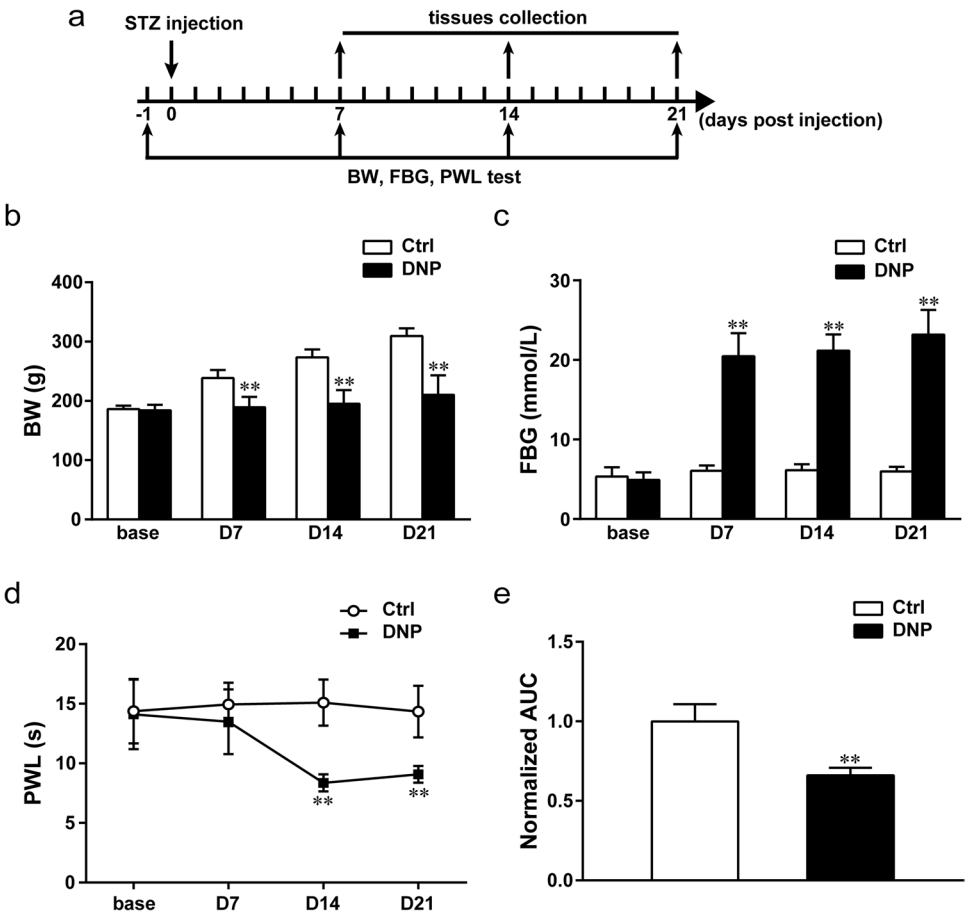

Fig. 1 Establishment of the DNP rat model. **a** Schematic representation of the process of establishing the DNP rat model. **b** Time course effect of STZ injection on BW. **c** Time course effect of STZ injection on FBG. **d** Time course effect of STZ injection on **PWL**. **e** Normalized area under the curve (AUC) analysis of **d**. AUC was standardized to the Ctrl group. Data are given as mean ± SD, $n = 16$ per group. $^{**}P < 0.01$ vs. Ctrl group

Fasting blood glucose and body weight measurement

FBG was measured using a glucometer (ACCU-CHEK Performa, Roche Diagnostics GmbH, Germany) at 1 day before STZ administration and 7, 14, and 21 days after STZ administration. BW was taken after starving the rats for 12 h followed by blood collection from the tail vein for FBG measurement.

Paw withdrawal latency test

PWL was evaluated by measuring hind paw withdrawal from a heat stimulus using a plantar test (37,370, Ugo Basile, Italy). PWL tests in experiment types 1 and 3 were done at 1 day before STZ inoculation and then 7, 14, and 21 days after STZ injection (Fig. 1a, Fig. 6a). In experiment type 2, the PWL test was done as outline in Fig. 5a. Before testing, rats were acclimated to individual Plexiglas cubicles on a glass plate for at least 30 min. The cutoff time was then set at 30 s and the radiant heat at 40 to avoid injury to rats. The light beam was switched off and timing stopped upon paw withdrawal. Each rat was tested independently thrice, at 5-min intervals, and PWL given by mean latencies, expressed in seconds.

RT-qPCR analysis

After deep anesthesia using sodium pentobarbital (80 mg/kg, i.p.), bilateral DRGs from L4 to L6 of rats were collected and stored in trizol (Invitrogen Corporation, USA) at − 80 °C, followed by total RNA extraction according to trizol manufacturer instructions. Next, cDNA was generated from 2 μg of total RNA with the RevertAid First Strand cDNA synthesis kit (#K1622, Thermo, USA) and stored at − 80 °C. Gene expression was then analyzed by real-time quantitative polymerase chain reactions (RT-qPCRs) on an ABI Stepone plus RT-PCR system using glyceraldehyde-3-phosphate dehydrogenase (GAPDH) as reference gene. The following primers were used: GAPDH: forward 5′-CTGGAGAAACCTGCCAAGTATG-3′; reverse 5′-GGTGGAAGAATGGGAGTTGCT-3′; P2X1: forward 5′-GGTGGGAGTCATTTTCCGTCT-3′; reverse 5′-CTGATGAGGTCACTTGAGGTCTG-3′; P2X2: forward 5′-GGGCAGTGTAGTCAGCATCAT-3′; reverse 5′-TCAGAAGTTCCATCCTCCACC-3′; P2X4: forward 5′-GAAAAGGGCTACCAGGAAACG-3′; reverse 5′-TCAGGAATCTCTGGACAG

GTGC-3′; P2X5: forward 5′-GGTTTGTGCTGTCTCTGT TCG-3′; reverse 5′-CCCAAGCATCGTGGTGTTAGT-3′; P2X6: forward 5′-TGCCTTAGATACCTGGGACAAC-3′; reverse 5′-GAGCAGTCAGAGCCTTTCGT-3′; P2X7: forward 5′-CTGGCTACAACTTCAGATACGC-3′; reverse 5′-GCCAAACCGAAATAGGACAGG-3′. The reaction was done in a final reaction volume of 15 μL comprised of 7.5 μL FastStart Universal SYBR Green Master (04,913 914 001, Roche, Germany), 1.5 μL sense and anti-sense primers (400 nM), 2 μL template cDNA, and 4 μL ribonuclease/deoxyribonuclease-free water. The reactions program was 95 °C for 10 min, followed by 40 cycles at 95 °C for 15 s. The reaction was then held at 60 °C for 60 s and of 60–95 °C melting curves generated. Each sample was analyzed in triplicate. Primer specificity was evaluated using melting curves and gel electrophoreses analysis. The $2^{-\Delta\Delta Ct}$ method was adopted to determine relative expression levels.

Western blot analysis

After deep anesthesia with sodium pentobarbital (80 mg/kg, i.p.), bilateral L4–L6 DRGs were collected and kept at − 80 °C. To extract protein, tissues were minced using ophthalmic scissors on ice in RIPA Lysis Buffer (P0013B, Beyotime, China) enriched with protease inhibitors (P1050, Beyotime, China), sonicated, the homogenate cleared by centrifugation at 12,000 rpm at 4 °C for 20 min, and then collected the supernatants. The supernatants were diluted with 2 × loading buffer, protein concentration determined using BCA Protein Assay Kit (23,225, Thermo Fisher, USA), and then denatured at 100 °C for 3 min. Proteins (20 μg) of each sample were fractionated with SDS-PAGE gels electrophoresis, transfer-embedded onto polyvinylidene difluoride membranes, and blocked with 5% nonfat milk in 1 × TBST (pH 7.5) for 1 h. They were then inoculated overnight with rabbit anti-P2X2 (1:1000, APR-003, Alomone, Israel), rabbit anti-P2X4 (1:1000; GTX54851, Gene Tex, USA), rabbit anti-P2X7 (1:1000; APR-004, Alomone, Israel), and β-actin (HRP conjugate, 1:5000; 12,262, Cell Signaling Technology, USA) at 4 °C. After rinsing thrice in 1 × TBST, 10 min each, the membrane for β-actin was visualized by chemiluminescence (ECL Plus; Beyotime, China), while the membranes for P2X2, P2X4, and P2X7 were incubated with HRP-linked antibody (1:5000; 7074, Cell Signaling technology, USA) for 2 h at room temperature and then washed with 1 × TBST and developed by chemiluminescence. Band intensities were quantified on an Image Quant LAS 4000 system. Target protein contents were normalized against β-actin content. Image J software was adopted to analyze the optical densities of the target proteins and β-actin. And then obtaining the relative expression amount of the target protein, namely the ratio of the gray value of the target protein to the gray value of β-actin.

Immunofluorescence

Rats were anesthetized using sodium pentobarbital (80 mg/kg, i.p.) and transcardially perfused with saline (4 °C) followed by 4% paraformaldehyde. The L4–L6 DRGs were then removed and post-fixed in 4% paraformaldehyde for 4 h. They were then dehydrated with 15% sucrose solution for 24 h and 30% for 48 h (until DRGs sank into the sucrose solution). The DRGs were then sectioned at 10 μm using a frozen microtome and placed on glass slides. After that, sections were rinsed thrice with 1 × TBST (pH 7.4), 10 min per wash, and blocked using 10% donkey serum in 1 × TBST for 1 h at 37 °C. They were then incubated overnight with rabbit anti-P2X4 (1:200, APR-002, Alomone, Israel) and rabbit anti-P2X7 (1:500, GTX104288, Gene Tex, USA) at 4 °C. They were washed 6 times with 1 × TBST (10 min each) and then incubated with Alexa Fluor 488 donkey anti-rabbit IgG (1:400; Jackson, 711–545-152) for 1 h at 37 °C. They were then sealed using antifade solution and cover glass and imaged on an Imager M2 microscope (ZEISS, Germany). The number of positive cells was calculated. Three sections per rat (3 rats from each group) were analyzed.

Drug administration

TNP-ATP (2464, Tocris, USA) was diluted to desired concentrations in freshly 0.9% NS before administration. TNP-ATP was administered into DNP + TNP-ATP 50 nmol (50 μL, 50 nmol) and DNP + TNP-ATP 100 nmol groups (50 μL, 100 nmol) through subcutaneous injection at dorsum of foot (left hind paw) from D15 to D21, once a day. Ctrl + NS and DNP + NS group rats received an equal volume of NS.

EA treatment

Rats in DNP + EA group were treated with 2 Hz EA daily for 7 consecutive days. The acupuncture needle (0.25 mm * 13 mm, Hua tuo, Suzhou Medical Appliance Manufactory, Jiangsu, China) was inserted into bilateral Zusanli (ST36, posterior lateral to the knee joint and about 5 mm below the capitulum fibulae) and Kunlun (BL60, depression between lateral malleolus and Achilles tendon of the hind limb) acupoints of rats. Then the needles were connected to HANS acupoint electrical stimulation device (Hans-200A, Jisheng Medical Technology, Beijing, China) for 30 min, setting with 1 mA and 2 Hz. Rats in other groups received same calming procedure without EA.

Statistical analysis

Data were given as mean ± standard deviation (SD) and analyzed on SPSS 22.0 (IBM, USA). Comparisons between 2 groups were done using independent sample *t* tests.

Comparisons among 3 (or over 3) groups were done using one-way ANOVA followed by LSD or Dunnett's post hoc tests, with $P < 0.05$ signifying statical significance.

Results

Establishment of a STZ-induced model of DNP

A type 1 diabetes model was developed via i.p. injection of high-dose STZ (65 mg/kg) and development of pain sensitization determined by behavioral testing (Fig. 1a). Compared to the Ctrl group, DNP rats exhibited remarkably higher FBG and lower BW 7 days after STZ injection (Fig. 1b,c, $P < 0.01$, respectively). PWL of DNP rats was remarkably reduced on D14 and this phenomenon remained to the end of the experiment (Fig. 1d, $P < 0.01$, respectively). Area under the curve (AUC) analysis revealed that PWL was remarkably lower in DNP group in contrast with the Ctrl group (Fig. 1e, $P < 0.01$). These data indicated that the DNP model was successfully established on D14.

Change in mRNA content of P2X receptors at various DNP stages

RT-qPCR analysis of P2X1-2, and P2X4-7 mRNA expression in rat DRGs at different stages after STZ administration revealed that in contrast with the Ctrl group, P2X2 and P2X4 were remarkably upregulated on D7 (Fig. 2b,c, $P < 0.01$, respectively), while P2X7 was remarkably elevated on D14 (Fig. 2f, $P < 0.01$). However, in contrast with the Ctrl group, P2X2 mRNA expression lost its difference on D21 (Fig. 2b, $P > 0.05$), while P2X4 and P2X7 mRNA expression remained consistently higher compared to Ctrl group (Fig. 2c,f, $P < 0.01$, respectively).

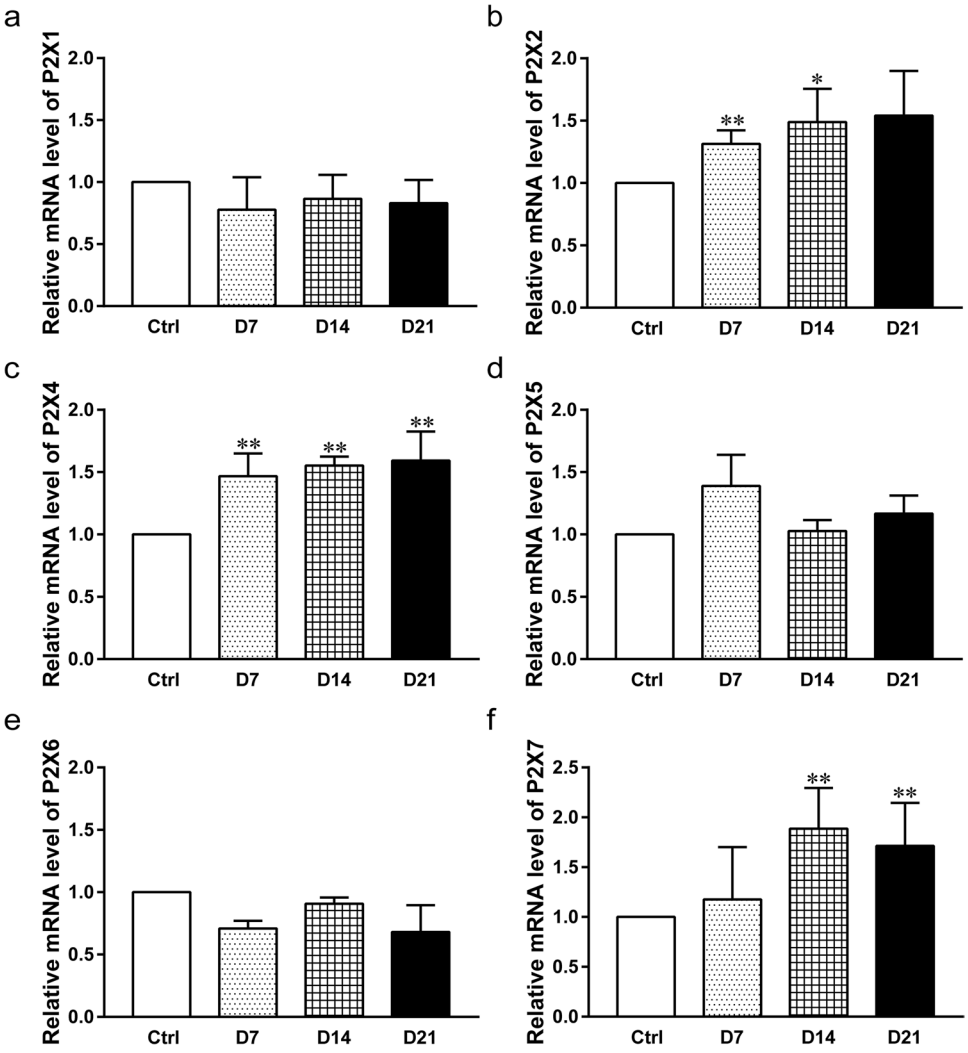

Fig. 2 P2X mRNA content in DRG of the rat DNP model at various timepoints **a**–**f** mRNA content of P2X1, P2X2, P2X4, P2X5, P2X6, and P2X7 in DRG of rats from various groups. Data are given as mean ± SD, $n = 5$–6 per group. $^{*}P < 0.05$, $^{**}P < 0.01$ vs. Ctrl group

Expression of P2X2, P2X4, and P2X7 in rat DRG at various DNP stages

Next, we used WB and IF to evaluate the protein content of P2X2, P2X4, and P2X7 in DRG from DNP rats (Figs. 3 and 4). WB analysis revealed that in contrast with the Ctrl group, the contents of P2X4 and P2X7 were markedly elevated on D21 (Fig. 3d,f, $P < 0.01$, respectively), while P2X4 was also evaluated on D14 (Fig. 3d, $P < 0.05$). However, P2X2 protein content did not differ remarkably in DRG of DNP rats in contrast with the Ctrl group (Fig. 3b, $P > 0.05$). IF analysis revealed that in contrast with Ctrl group, DNP rats had significantly higher P2X4 expression on D7, which persisted to D21 (Fig. 4b, $P < 0.01$, respectively), while P2X7 expression in DRG was elevated on D14 and persisted to D21 (Fig. 4c, $P < 0.01$, respectively).

Effects of single and multiple TNP-ATP injections in different doses on DNP rats

We verified the involvement of P2X4 and P2X7 in the process of DNP via single and multiple TNP-ATP subcutaneous injections at dorsum of foot and then measured the PWL changes (Fig. 5). At 15 days after STZ administration, TNP-ATP was administered into rats at left hind paw with two doses (50 nmol, 100 nmol) and BW, FBG, and PWL were measured as outline in Fig. 6a. This analysis illustrated that in contrast with the DNP + NS group, BW and FBG in DNP rats were not affected by TNP-ATP at both doses (Fig. 5b,c $P > 0.05$, respectively). Next, we examined PWL at 0.5 h, 1 h, and 1.5 h after TNP-ATP administration on D15 and found that in contrast with the DNP + NS group, 100 nmol TNP-ATP increased PWL at 0.5 h after injection (Fig. 5d, $P < 0.05$), but 50 nmol of TNP-ATP did not change the PWL (Fig. 5d, $P > 0.05$). To determine if repetitive TNP-ATP administrations affect PWL, we treated the DNP rats with TNP-ATP (50 nmol and 100 nmol) daily from D15 to D21 (Fig. 5a). This analysis illustrated that in contrast with DNP + NS group, repetitive administrations of 100 nmol TNP-ATP remarkably increased the PWL of DNP rats on D21 (Fig. 5e, $P < 0.01$), but 50 nmol dose did not affect PWL in DNP rats (Fig. 5e, $P > 0.05$).

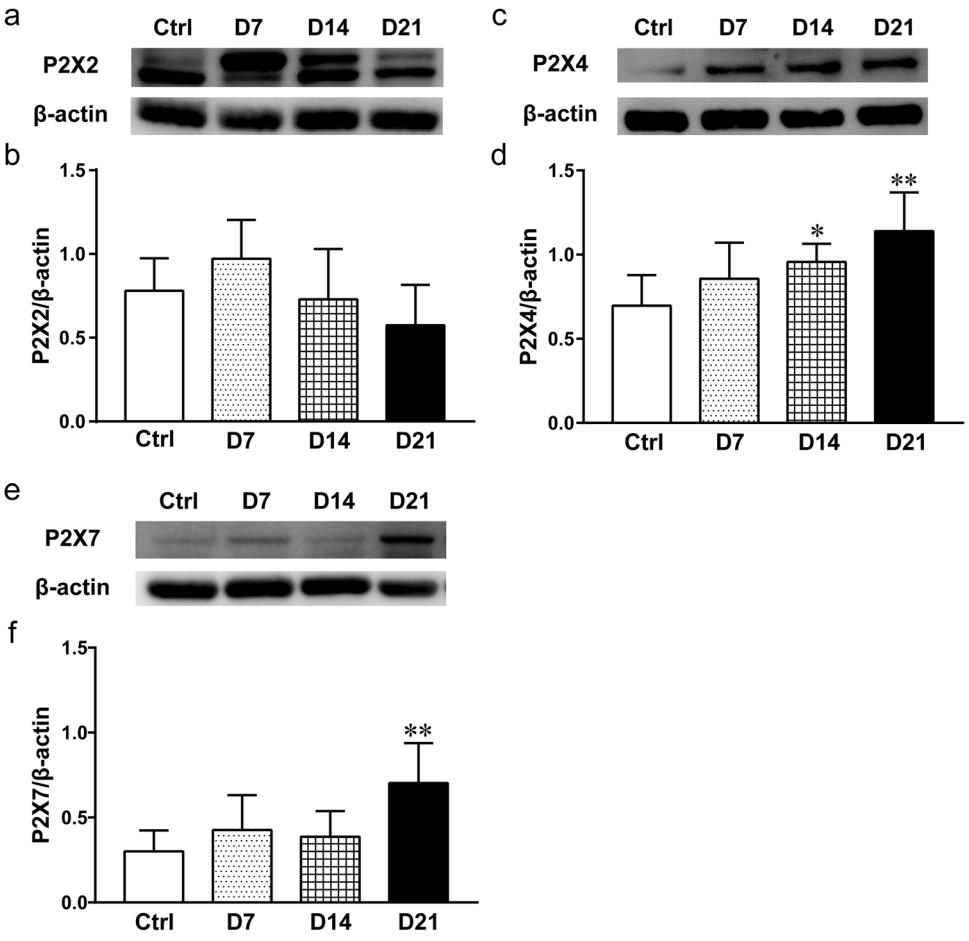

Fig. 3 Protein content of P2X2, P2X4, and P2X7 in rat DRG after STZ injection at various timepoints. **a** Representative images of P2X2 protein content in DRG. **b** Relative P2X2 protein level in DRG of rats from various groups. **c** Representative images of P2X4 protein content in DRG. **d** Relative P2X4 protein level in DRG of rats from various groups. **e** Representative images of P2X7 protein content in DRG. **f** Relative P2X7 protein level in DRG of rats from various groups. Data are given as mean ± SD, $n = 5$ per group. $^{*}P < 0.05$, $^{**}P < 0.01$ vs. Ctrl group

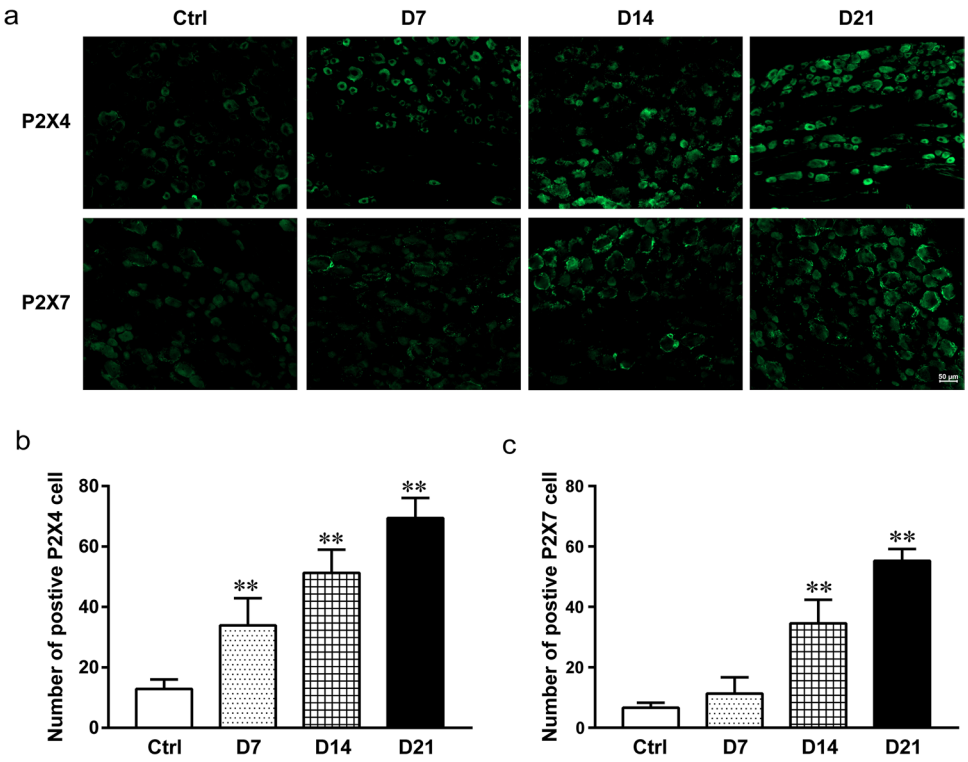

Fig. 4 Immunofluorescence analysis of P2X4 and P2X7 levels in DRG of DNP rats at various timepoints. **a** Representative images of P2X4 and P2X7 staining in DRGs from various groups. **b** Quantification of P2X4 positive cells in DRG of rats from various groups. **c** Quantification of P2X7 positive cells in DRG of rats from various groups. Scale bars = 50 μm. Data are given as mean ± SD, $n = 3$ per group. $^{**}P < 0.01$ vs. Ctrl group

EA relieves thermal hyperalgesia in DNP rats

Next, we treated STZ-induced DNP rats with EA for 7 consecutive days as outline in Fig. 6a. This analysis revealed that in contrast with the Ctrl group, rats in DNP and DNP + EA groups exhibited lower PWL at 14 days after STZ administration (Fig. 6d, $P < 0.01$, respectively). EA treatment for 7 days increased PWL in contrast with DNP rats on D21 (Fig. 6d, $P < 0.01$). AUC analysis of PWL from D14 to D21 exhibited the overall impact of EA on thermal hyperalgesia in DNP rats (Fig. 6e, $P < 0.01$). In contrast with the DNP group, EA did not affect BW and FBG in DNP rats (Fig. 6b,c, $P > 0.05$, respectively).

EA reduces the mRNA level of P2X4 and P2X7 in DRG of DNP rats

RT-qPCR analysis of P2X4 and P2X7 mRNA expression in DRG after EA treatment for 7 days revealed that both remarkably upregulated in DRG of DNP rats in contrast with Ctrl group (Fig. 7a,d, $P < 0.01$ for P2X4, $P < 0.05$ for P2X7), and that EA treatment reduced their mRNA expression in contrast with the DNP group (Fig. 7a,d, $P < 0.05$, respectively).

EA reduces P2X4 and P2X7 expression in DRG of DNP rats

Next, we used WB and IF to assess if EA treatment for 7 days affects the protein content of P2X4 and P2X7 in DRG of DNP rats (Figs. 8 and 9). WB analysis revealed that in contrast with the Ctrl group, P2X4 and P2X7 protein expressions were elevated in DNP group (Fig. 8b,d, $P < 0.01$ for P2X7, $P < 0.05$ for P2X4), while EA treatment reduced P2X4 and P2X7 protein expression in DNP + EA group in contrast with DNP group (Fig. 8b,d, $P < 0.05$, respectively). IF analysis revealed that DNP rats had higher P2X4 and P2X7 expression levels in DRG in contrast with Ctrl group (Fig. 9b,c, $P < 0.01$, respectively), and that EA treatment markedly inhibited their expression in contrast with DNP group (Fig. 9b,c, $P < 0.01$, respectively).

Discussion

STZ-induced diabetes recapitulates various aspects of human diabetes, entailing insulin deficiency, weight loss, and hyperglycemia [29, 30], and is also widely used in the investigation of the mechanisms underlying DNP and potential therapies. Here, we generated a rat model of DNP by intraperitoneally injecting with a single large dose of STZ (65 mg/kg). Our findings showed that at 7 days after STZ administration, the FBG of the DNP group rats increased and the BW decreased. And the PWL in DNP group rats reduced at 14 days post STZ administration, indicating successful generation of DNP rat model.

Chronic neuropathic pain often begins with peripheral nerve injury. Once the initial irritant injury occurs, a cascade of inflammatory mediators will be activated peripherally and

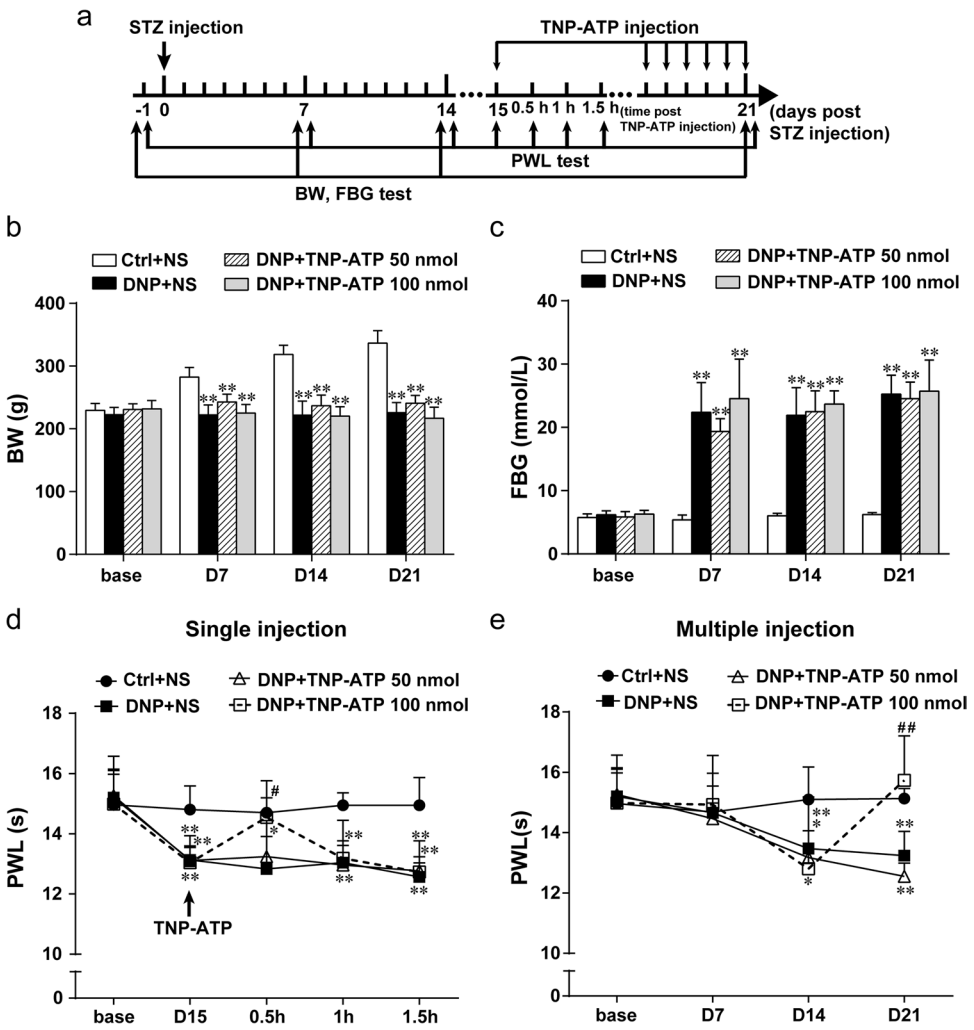

Fig. 5 Effects of various TNP-ATP doses on PWL in DNP rats. **a** Schedule for TNP-ATP treatment. **b** Time course effect of STZ and TNP-ATP on BW. **c** Time course effect of STZ and TNP-ATP on FBG. **d** Effect of the single administration of 50 and 100 nmol TNP-ATP on PWL in DNP rats. **e** Effect of the multiple administrations of 50 and 100 nmol TNP-ATP on PWL in DNP rats. Data are given as mean ± SD, $n = 6$ per group. $^{*}P < 0.05$, $^{**}P < 0.01$ vs. Ctrl + NS group. $^{\#}P < 0.05$, $^{\#\#}P < 0.01$ vs. DNP + NS group

centrally [31]. The DRG, which is located at the junction of the peripheral and central nervous system, is an ideal target for pain control [32]. P2X receptors are ligand-gated ion channels (Na^+, K^+, and Ca^{2+}) which regulate rapid response [33]. These receptors can be activated by ATP, leading to intercellular communication and inflammatory transmission [34]. Ionotropic P2X receptors are reported to be involved in pain signaling under physiologic conditions [35]. Until now, the relationship between P2X3, P2X4, P2X7, and pain sensitization is clearer than other subtypes [36–38]. However, it is not clear if P2X1, P2X2, P2X5, and P2X6 receptors in DRG are involved in neuropathic pain.

P2X1 receptor has been implicated in the development of thrombotic inflammatory diseases [39]. The ATP-activated P2X2, P2X4, and P2X6 receptors in the 2nd layer of the spinal cord are involved in the transmission of nociceptive information [40], while in spinal dorsal horn, has been proven [41]. In addition, P2X5 has been implicated in peripheral pain [42]. We have previously shown that in DRG, P2X3 takes part in the development of DNP [17, 18]. Here, analysis of the mRNA content of P2X1–2 and P2X4–7 receptors in DRG at different DNP stages revealed that the mRNA levels of P2X2, P2X4, and P2X7 receptors were increased in DNP rats. Both WB and IF results showed that P2X4 and P2X7 protein contents were increased but P2X2 did not change remarkably. These results are consistent with previous findings [43, 44].

TNP-ATP is a nonspecific P2X receptor antagonist that inhibits all P2X receptors [45, 46]. Intrathecal injection of TNP-ATP is reported to block tactile allodynia triggered by L5 nerve injury and to inhibit P2X4 activation in microglia [47]. TNP-ATP has also been shown to inhibit chicken P2X7 receptor and chicken P2X7 receptor-associated current has been shown to have similar properties to those P2X7 receptors in other animals [48]. To determine if the P2X4 and P2X7 in DRG were involved in thermal hyperalgesia in DNP rats, we administered single and multiple injections of various doses of TNP-ATP into the dorsum of the foot and found that single and multiple injections of TNP-ATP at high dose (100 nmol), but not the low dose (50 nmol),

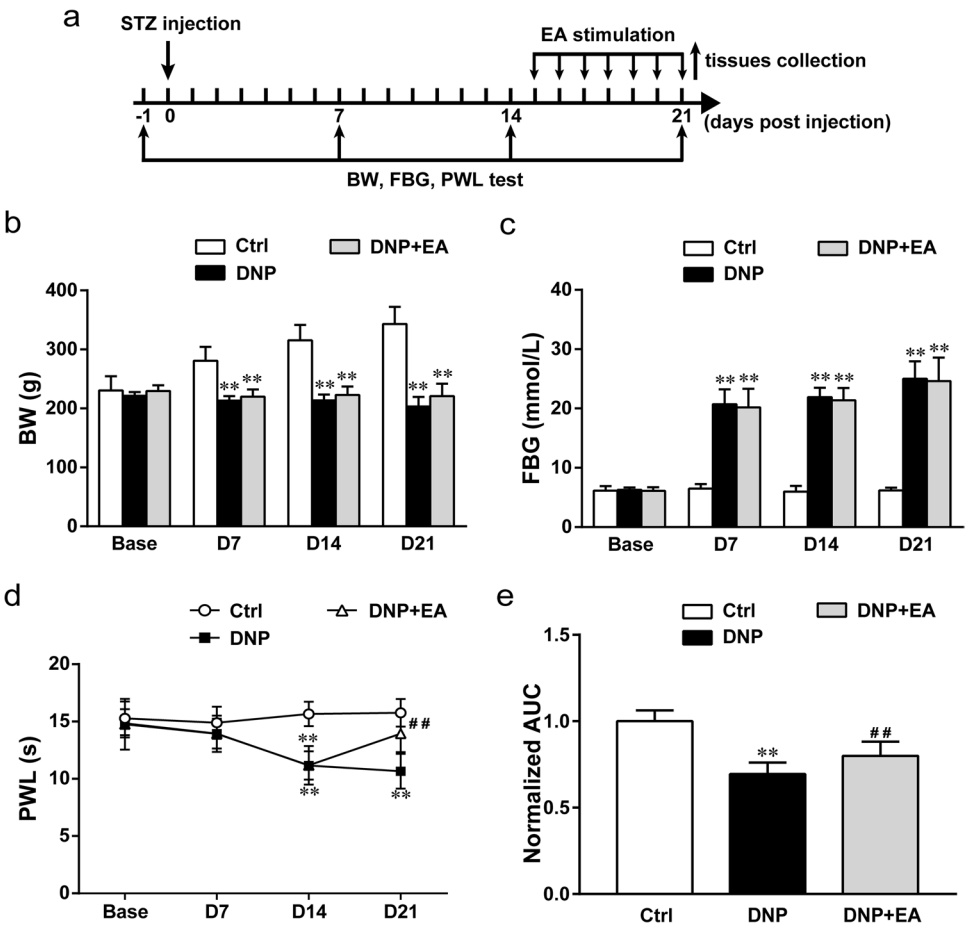

Fig. 6 Effect of EA on PWL in DNP rats. **a** Schedule of DNP rat model establishment and EA treatment. **b** Time course effect of STZ and EA treatment on BW. **c** Time course effect of STZ and EA treatment on FBG. **d** Analgesic effects of EA on PWL. **e** Normalized AUC analysis for D14 to D21 of **d**. Data are given as mean ± SD, $n = 16$ per group. $^{*}P < 0.01$ vs. Ctrl group. $^{\#\#}P < 0.01$ vs. DNP group

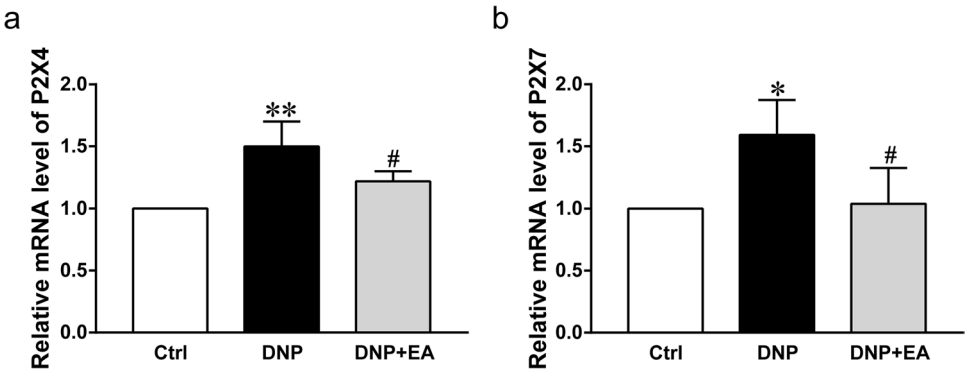

Fig. 7 Effect of EA on the mRNA levels of P2X4 and P2X7 in DRG. **a** mRNA level of P2X4 in DRG of rats from various groups. **b** mRNA level of P2X7 in DRG of rats from various groups. Data are given as mean ± SD, $n = 5$–6 per group. $^{*}P < 0.05$, $^{**}P < 0.01$ vs. Ctrl group. $^{\#}P < 0.05$ vs. DNP group

reversed DNP-induced pain sensitization. Thus, TNP-ATP dose dependently reduced thermal hyperalgesia in DNP rats. Altogether, these findings illustrate that elevated expression of P2X4 and P2X7 may contribute to diabetes-induced hyperalgesia.

The extensive application of electroacupuncture has been proven by multifaceted research, especially in the aspect of analgesia [49–52]. Studies show that EA relieves pain by regulating signaling pathways and inflammatory cytokines [53, 54]. However, it is not clear if EA influences hyperpathia in DNP rats by regulating P2X4 and P2X7 in DRG. Because the DNP rat model was successfully established at 14 days after STZ injection, we performed EA treatment from 15 to 21 days after STZ injection. The results show that EA increased the PWL in DNP rats and reduces the expression of P2X4 and P2X7 in DRG. Our data indicate that EA may relieve DNP by regulating P2X4 and P2X7 in DRG.

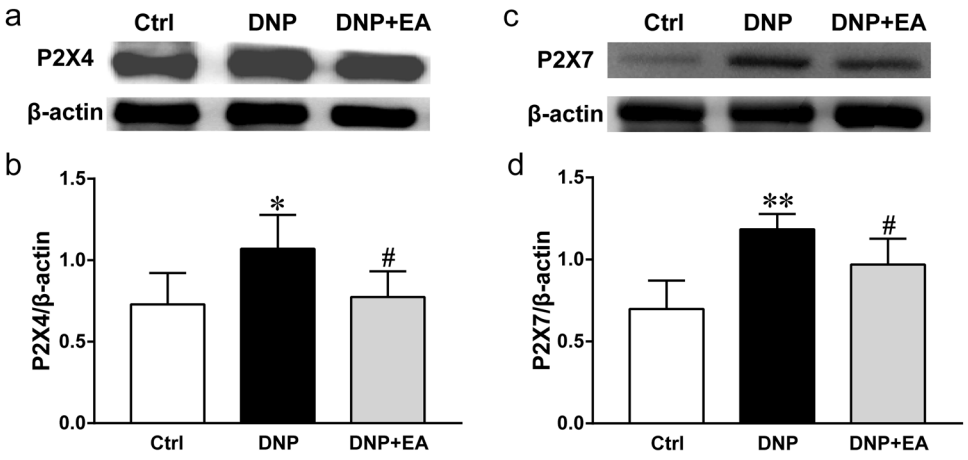

Fig. 8 Effect of EA on the protein level of P2X4 and P2X7 in DRG. **a** Representative images of P2X4 protein level in DRG. **b** Relative P2X4 protein level in DRG of rats from various groups. **c** Representative images of P2X7 protein level in DRG. **d** Relative P2X7 protein level in DRG of rats from various groups. Data are given as mean ± SD, $n = 5$ per group. $^{*}P < 0.05$, $^{**}P < 0.01$ vs. Ctrl group. $^{\#}P < 0.05$ vs. DNP group

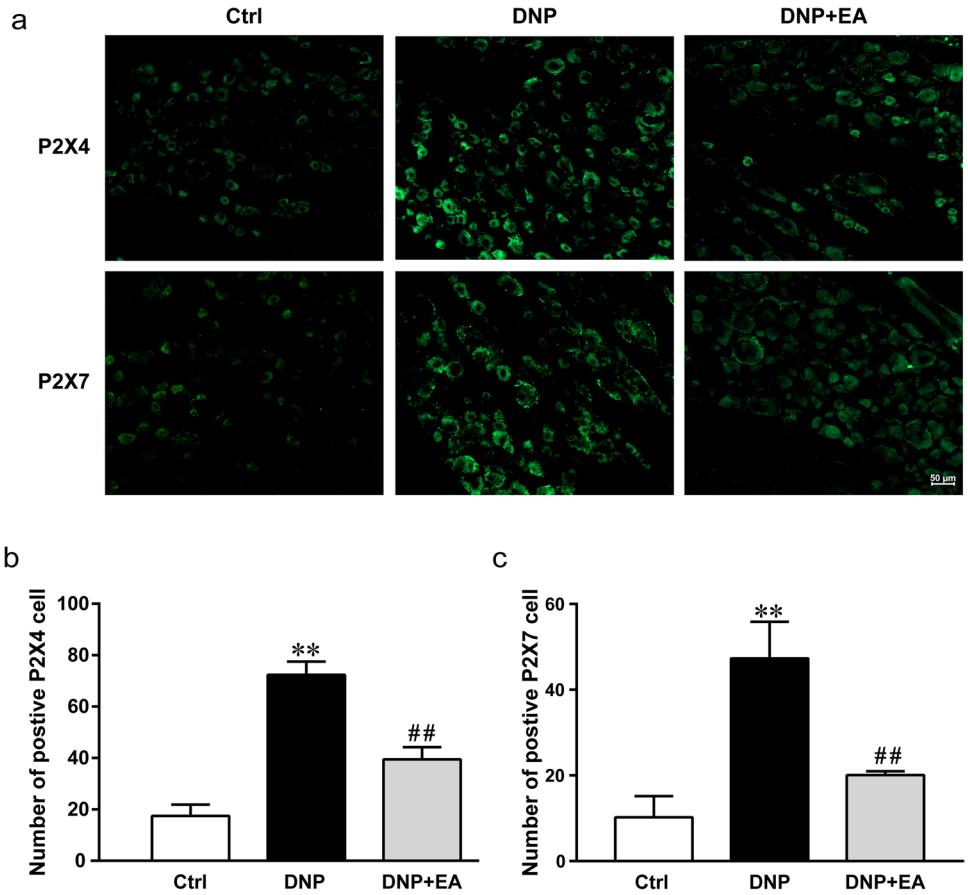

Fig. 9 Effect of EA treatment on P2X4 and P2X7 levels in DRG. **a** Representative IF images of P2X4 and P2X7 in DRG from various groups. **b** Quantification of P2X4 positive cells in rat DRGs from various groups. **c** Quantification of P2X7 positive cells in rat DRGs from various groups. Scale bars = 50 μm. Data are given as mean ± SD, $n = 3$ per group. $^{**}P < 0.01$ vs. Ctrl group. $^{\#\#}P < 0.01$ vs. DNP group

Conclusions

In summary, our results indicate that activation of P2X4 and P2X7 in L4–L6 DRGs contributes to diabetes-induced hyperalgesia and that EA may ameliorate pain hypersensitivities in a rat model of DNP by suppressing P2X4 and P2X7 upregulation in DRG. Our findings highlight the therapeutic potential of EA in clinical DNP management.

Author contribution Xiao Fen He, Yongliang Jiang, and Jianqiao Fang conceived of and designed the experiments. Yurong Kang, Hanzhi

Wang, and Siying Qu performed the animal experiments. Xiao Fen He, Hanzhi Wang, Siying Qu, and Xiang Li performed immunofluorescence. Luhang Chen, Liqian Ma, and Qunqi Hu performed WB and PCR. Boyu Liu, Yi Liang, Junfan Fang, and Xiaomei Shao analyzed the data. Qunqi Hu, Xiaofen He, and Yiqi Ma wrote the manuscripts. Qunqi Hu and Yiqi Ma participated in figures preparations. All authors read and approved the final manuscript.

Funding This research was supported by the National Natural Science Foundation of China (81804181 to X.F.H. and 81774389 to Y.L.J.), the National Undergraduate Innovation and Entrepreneurship Training Program (202110344013), and the Key Laboratory of Acupuncture and Neurology of Zhejiang Province (2019E10011).

National Natural Science Foundation of China,81774389,Yong-Liang Jiang,81804181,Xiao-fen He,National Undergraduate Innovation and Entrepreneurship Training Program,202110344013,Xiang Li

Data availability The datasets generated during and/or analyzed during the current study are available from the corresponding author on reasonable request.

Declarations

Conflicts of interest The authors declare no competing interests.

Ethical approval The study was approved by the ethics committee of Zhejiang Chinese Medical University, Hangzhou, China (Approval No. IACUC-20190805–04).

References

1. Tabish SA (2007) Is diabetes becoming the biggest epidemic of the twenty-first century? Int J Health Sci (Qassim) 1(2):V-viii.
2. Ogurtsova K, da Rocha Fernandes JD, Huang Y, Linnenkamp U, Guariguata L, Cho NH, Cavan D, Shaw JE, Makaroff LE (2017) IDF diabetes atlas: global estimates for the prevalence of diabetes for 2015 and 2040. Diabetes Res Clin Pract 128:40–50. https://doi.org/10.1016/j.diabres.2017.03.024
3. Rahimi-Madiseh M, Malekpour-Tehrani A, Bahmani M, Rafieian-Kopaei M (2016) The research and development on the antioxidants in prevention of diabetic complications. Asian Pac J Trop Med 9(9):825–831. https://doi.org/10.1016/j.apjtm.2016.07.001
4. Magadmi RM, Alsulaimani MA, Al-Rafiah AR, Ahmad MS, Esmat A (2021) Carvedilol exerts neuroprotective effect on rat model of diabetic neuropathy. Front Pharmacol 12:613634. https://doi.org/10.3389/fphar.2021.613634
5. Smith HS, Argoff CE (2011) Pharmacological treatment of diabetic neuropathic pain. Drugs 71(5):557–589. https://doi.org/10.2165/11588940-000000000-00000
6. Alberti KG, Zimmet PZ (1998) Definition, diagnosis and classification of diabetes mellitus and its complications. Part 1: diagnosis and classification of diabetes mellitus provisional report of a WHO consultation. Diabet Med 15(7):539–553. https://doi.org/10.1002/(sici)1096-9136(199807)15:7<539::aid-dia668>3.0.co;2-s
7. Coppini DV (2016) Enigma of painful diabetic neuropathy: can we use the basic science, research outcomes and real-world data to help improve patient care and outcomes? Diabet Med 33(11):1477–1482. https://doi.org/10.1111/dme.13089
8. Impellizzeri D, Peritore AF, Cordaro M, Gugliandolo E, Siracusa R, Crupi R, D'Amico R, Fusco R, Evangelista M, Cuzzocrea S, Di Paola R (2019) The neuroprotective effects of micronized PEA (PEA-m) formulation on diabetic peripheral neuropathy in mice. Faseb j 33(10):11364–11380. https://doi.org/10.1096/fj.201900538R
9. D'Amico R, Impellizzeri D, Cuzzocrea S, Di Paola R (2020) ALIAmides update: palmitoylethanolamide and its formulations on management of peripheral neuropathic pain. Int J Mol Sci 21(15). https://doi.org/10.3390/ijms21155330
10. Kaczmarek-Hájek K, Lörinczi E, Hausmann R, Nicke A (2012) Molecular and functional properties of P2X receptors—recent progress and persisting challenges. Purinergic Signal 8(3):375–417. https://doi.org/10.1007/s11302-012-9314-7
11. Khakh BS, North RA (2006) P2X receptors as cell-surface ATP sensors in health and disease. Nature 442(7102):527–532. https://doi.org/10.1038/nature04886
12. Bleehen T, Keele CA (1977) Observations on the algogenic actions of adenosine compounds on the human blister base preparation. Pain 3(4):367–377. https://doi.org/10.1016/0304-3959(77)90066-5
13. Huang Z, Xie N, Illes P, Di Virgilio F, Ulrich H, Semyanov A, Verkhratsky A, Sperlagh B, Yu SG, Huang C, Tang Y (2021) From purines to purinergic signalling: molecular functions and human diseases. Signal Transduct Target Ther 6(1):162. https://doi.org/10.1038/s41392-021-00553-z
14. He YQ, Lang XQ, Lin L, Ji L, Yuan XY, Chen Q, Ran YM, Chen HS, Li L, Wang JM, Wang ZG, Gregersen H, Zou DW, Liang HP, Yang M (2017) P2X3 receptor-mediated visceral hyperalgesia and neuronal sensitization following exposure to PTSD-like stress in the dorsal root ganglia of rats. Neurogastroenterol Motil 29(3). https://doi.org/10.1111/nmo.12976
15. Cook SP, Vulchanova L, Hargreaves KM, Elde R, McCleskey EW (1997) Distinct ATP receptors on pain-sensing and stretch-sensing neurons. Nature 387(6632):505–508. https://doi.org/10.1038/387505a0
16. D'Amico R, Fusco R, Siracusa R, Impellizzeri D, Peritore AF, Gugliandolo E, Interdonato L, Sforza AM, Crupi R, Cuzzocrea S, Genovese T, Cordaro M, Di Paola R (2021) Inhibition of P2X7 purinergic receptor ameliorates fibromyalgia syndrome by suppressing NLRP3 pathway. Int J Mol Sci 22(12). https://doi.org/10.3390/ijms22126471
17. Fei X, He X, Tai Z, Wang H, Qu S, Chen L, Hu Q, Fang J, Jiang Y (2020) Electroacupuncture alleviates diabetic neuropathic pain in rats by suppressing P2X3 receptor expression in dorsal root ganglia. Purinergic Signal 16(4):491–502. https://doi.org/10.1007/s11302-020-09728-9
18. Zhou YF, Ying XM, He XF, Shou SY, Wei JJ, Tai ZX, Shao XM, Liang Y, Fang F, Fang JQ, Jiang YL (2018) Suppressing PKC-dependent membrane P2X3 receptor upregulation in dorsal root ganglia mediated electroacupuncture analgesia in rat painful diabetic neuropathy. Purinergic Signal 14(4):359–369. https://doi.org/10.1007/s11302-018-9617-4
19. Snyder MJ, Gibbs LM, Lindsay TJ (2016) Treating painful diabetic peripheral neuropathy: an update. Am Fam Physician 94(3):227–234
20. Peltier A, Goutman SA, Callaghan BC (2014) Painful diabetic neuropathy Bmj 348:g1799. https://doi.org/10.1136/bmj.g1799
21. Heo I, Shin BC, Cho JH, Ha IH, Hwang EH, Lee JH, Kim KW, Kim MR, Jung SY, Kwon O, Kim NK, Son DW, Shin KM (2021) Multicentre randomised controlled clinical trial of electroacupuncture with usual care for patients with non-acute pain after back surgery. Br J Anaesth 126(3):692–699. https://doi.org/10.1016/j.bja.2020.10.038
22. Arriaga-Pizano L, Gómez-Jiménez DC, Flores-Mejía LA, Pérez-Cervera Y, Solórzano-Mata CJ, López-Macías C, Isibasi A, Torres-Rosas R (2020) Low back pain in athletes can be controlled with acupuncture by a catecholaminergic pathway:

clinical trial. Acupunct Med 38(6):388–395. https://doi.org/10.1177/0964528420912251
23. Huang CZ, Li YL, Lan XL, He B, Yang J, Li J (2021) [Electroacupuncture combined with acupoint catgut embedding for postoperative pain after fistulotomy]. Zhen Ci Yan Jiu 46(5):421–425. https://doi.org/10.13702/j.1000-0607.200603
24. Lv ZT, Shen LL, Zhu B, Zhang ZQ, Ma CY, Huang GF, Yin J, Yu LL, Yu SY, Ding MQ, Li J, Yuan XC, He W, Jing XH, Li M (2019) Effects of intensity of electroacupuncture on chronic pain in patients with knee osteoarthritis: a randomized controlled trial. Arthritis Res Ther 21(1):120. https://doi.org/10.1186/s13075-019-1899-6
25. Manni L, Florenzano F, Aloe L (2011) Electroacupuncture counteracts the development of thermal hyperalgesia and the alteration of nerve growth factor and sensory neuromodulators induced by streptozotocin in adult rats. Diabetologia 54(7):1900–1908. https://doi.org/10.1007/s00125-011-2117-5
26. Zhou DM, Zhuang Y, Chen WJ, Li W, Miao B (2018) Effects of duloxetine on the toll-like receptor 4 signaling pathway in spinal dorsal horn in a rat model of diabetic neuropathic pain. Pain Med 19(3):580–588. https://doi.org/10.1093/pm/pnx125
27. Wang F, Ma J, Han F, Guo X, Meng L, Sun Y, Jin C, Duan H, Li H, Peng Y (2016) DL-3-n-butylphthalide delays the onset and progression of diabetic cataract by inhibiting oxidative stress in rat diabetic model. Sci Rep 6:19396. https://doi.org/10.1038/srep19396
28. Erbaş O, Oltulu F, Yılmaz M, Yavaşoğlu A, Taşkıran D (2016) Neuroprotective effects of chronic administration of levetiracetam in a rat model of diabetic neuropathy. Diabetes Res Clin Pract 114:106–116. https://doi.org/10.1016/j.diabres.2015.12.016
29. Kolb H (1987) Mouse models of insulin dependent diabetes: low-dose streptozocin-induced diabetes and nonobese diabetic (NOD) mice. Diabetes Metab Rev 3(3):751–778. https://doi.org/10.1002/dmr.5610030308
30. Wang-Fischer Y, Garyantes T (2018) Improving the reliability and utility of streptozotocin-induced rat diabetic model. J Diabetes Res 2018:8054073. https://doi.org/10.1155/2018/8054073
31. Berger AA, Liu Y, Possoit H, Rogers AC, Moore W, Gress K, Cornett EM, Kaye AD, Imani F, Sadegi K, Varrassi G, Viswanath O, Urits I (2021) Dorsal root ganglion (DRG) and chronic pain. Anesth Pain Med 11(2):e113020. https://doi.org/10.5812/aapm.113020
32. Esposito MF, Malayil R, Hanes M, Deer T (2019) Unique characteristics of the dorsal root ganglion as a target for neuromodulation. Pain Med 20(Suppl 1):S23-s30. https://doi.org/10.1093/pm/pnz012
33. Zou Y, Yang R, Li L, Xu X, Liang S (2021) Purinergic signaling: a potential therapeutic target for depression and chronic pain. Purinergic Signal. https://doi.org/10.1007/s11302-021-09801-x
34. Burnstock G (2017) Purinergic signalling: therapeutic developments Front Pharmacol 8:661. https://doi.org/10.3389/fphar.2017.00661
35. Burnstock G (2006) Purinergic P2 receptors as targets for novel analgesics. Pharmacol Ther 110(3):433–454. https://doi.org/10.1016/j.pharmthera.2005.08.013
36. Zhang WJ, Zhu ZM, Liu ZX (2020) The role and pharmacological properties of the P2X7 receptor in neuropathic pain. Brain Res Bull 155:19–28. https://doi.org/10.1016/j.brainresbull.2019.11.006
37. Duveau A, Bertin E, Boué-Grabot E (2020) Implication of neuronal versus microglial P2X4 receptors in central nervous system disorders. Neurosci Bull 36(11):1327–1343. https://doi.org/10.1007/s12264-020-00570-y
38. Krajewski JL (2020) P2X3-containing receptors as targets for the treatment of chronic pain. Neurotherapeutics 17(3):826–838. https://doi.org/10.1007/s13311-020-00934-2
39. Oury C, Lecut C, Hego A, Wéra O, Delierneux C (2015) Purinergic control of inflammation and thrombosis: role of P2X1 receptors. Comput Struct Biotechnol J 13:106–110. https://doi.org/10.1016/j.csbj.2014.11.008
40. Bardoni R, Goldstein PA, Lee CJ, Gu JG, MacDermott AB (1997) ATP P2X receptors mediate fast synaptic transmission in the dorsal horn of the rat spinal cord. J Neurosci 17(14):5297–5304. https://doi.org/10.1523/jneurosci.17-14-05297.1997
41. Zheng XB, Zhang YL, Li Q, Liu YG, Wang XD, Yang BL, Zhu GC, Zhou CF, Gao Y, Liu ZX (2019) Effects of 1,8-cineole on neuropathic pain mediated by P2X2 receptor in the spinal cord dorsal horn. Sci Rep 9(1):7909. https://doi.org/10.1038/s41598-019-44282-4
42. Kobayashi K, Yamanaka H, Noguchi K (2013) Expression of ATP receptors in the rat dorsal root ganglion and spinal cord. Anat Sci Int 88(1):10–16. https://doi.org/10.1007/s12565-012-0163-9
43. Yuan H, Ouyang S, Yang R, Li S, Gong Y, Zou L, Jia T, Zhao S, Wu B, Yi Z, Liu H, Shi L, Li L, Gao Y, Li G, Xu H, Liu S, Zhang C, Liang S (2018) Osthole alleviated diabetic neuropathic pain mediated by the P2X(4) receptor in dorsal root ganglia. Brain Res Bull 142:289–296. https://doi.org/10.1016/j.brainresbull.2018.08.008
44. Wang A, Shi X, Yu R, Qiao B, Yang R, Xu C (2021) The P2X(7) Receptor is involved in diabetic neuropathic pain hypersensitivity mediated by TRPV1 in the rat dorsal root ganglion. Front Mol Neurosci 14:663649. https://doi.org/10.3389/fnmol.2021.663649
45. Horvath RJ, DeLeo JA (2009) Morphine enhances microglial migration through modulation of P2X4 receptor signaling. J Neurosci 29(4):998–1005. https://doi.org/10.1523/jneurosci.4595-08.2009
46. Xiao J, Huang Y, Li X, Li L, Yang T, Huang L, Yang L, Jiang H, Li H, Li F (2016) TNP-ATP is beneficial for treatment of neonatal hypoxia-induced hypomyelination and cognitive decline. Neurosci Bull 32(1):99–107. https://doi.org/10.1007/s12264-015-0003-8
47. Tsuda M, Shigemoto-Mogami Y, Koizumi S, Mizokoshi A, Kohsaka S, Salter MW, Inoue K (2003) P2X4 receptors induced in spinal microglia gate tactile allodynia after nerve injury. Nature 424(6950):778–783. https://doi.org/10.1038/nature01786
48. Kasuya G, Yamaura T, Ma XB, Nakamura R, Takemoto M, Nagumo H, Tanaka E, Dohmae N, Nakane T, Yu Y, Ishitani R, Matsuzaki O, Hattori M, Nureki O (2017) Structural insights into the competitive inhibition of the ATP-gated P2X receptor channel. Nat Commun 8(1):876. https://doi.org/10.1038/s41467-017-00887-9
49. Gao F, Xiang HC, Li HP, Jia M, Pan XL, Pan HL, Li M (2018) Electroacupuncture inhibits NLRP3 inflammasome activation through CB2 receptors in inflammatory pain. Brain Behav Immun 67:91–100. https://doi.org/10.1016/j.bbi.2017.08.004
50. Chen H, Liu TY, Kuai L, Zhu J, Wu CJ, Liu LM (2013) Electroacupuncture treatment for pancreatic cancer pain: a randomized controlled trial. Pancreatology 13(6):594–597. https://doi.org/10.1016/j.pan.2013.10.007
51. He JR, Yu SG, Tang Y, Illes P (2020) Purinergic signaling as a basis of acupuncture-induced analgesia. Purinergic Signal 16(3):297–304. https://doi.org/10.1007/s11302-020-09708-z
52. Tang Y, Yin HY, Rubini P, Illes P (2016) Acupuncture-induced analgesia: a neurobiological basis in purinergic signaling. Neuroscientist 22(6):563–578. https://doi.org/10.1177/1073858416654453

53. Wang S, Du J, Shao F, Wang W, Sun H, Shao X, Liang Y, Liu B, Fang J, Fang J (2020) Electroacupuncture regulates pain transition by inhibiting the mGluR5-PKCε signaling pathway in the dorsal root ganglia. J Pain Res 13:1471–1483. https://doi.org/10.2147/jpr.s251948
54. Ali U, Apryani E, Wu HY, Mao XF, Liu H, Wang YX (2020) Low frequency electroacupuncture alleviates neuropathic pain by activation of spinal microglial IL-10/β-endorphin pathway. Biomed Pharmacother 125:109898. https://doi.org/10.1016/j.biopha.2020.109898